A Deep Approach for Reliable Subsurface Imaging in Software-Defined Ground Penetrating Radar

Bisma Amjad, Tauseef Tauqeer, Fahad Shamshad,
Rehan Hafiz, Mahboob Ur Rahman
Department of Electrical Engineering, Information Technology University, Lahore, Pakistan

Abstract

Software-Defined Radio (SDR) based Ground-Penetrating Radar (GPR) has emerged as an effective tool for subsurface imaging due to its flexible and non-invasive nature. However, the non-ideal behaviour of its components leads to phase distortions that eventually corrupts the acquired subsurface images. Unlike conventional signal processing techniques, this work aims to leverage the power of deep neural networks to effectively mitigate the phase distortions. We show the effectiveness of the proposed approach, GPRNet, via experiments on real subsurface imaging data acquired via SDR based GPR.

1 Introduction

Ground Penetrating Radar (GPR) serves as a primary geophysical tool that finds numerous applications in the field of earth sciences. Its non-invasive nature allows exploring the relevant geophysical aspects of the earth. Because of its diverse applications ranging from detecting landmines, to minerals detection, soil analysis, exploring water beds, and conducting archaeological surveys, reliable subsurface imaging methods using GPR have been gaining much attention in the geophysical community lately [1].

GPR works on the basic principle of echo detection. It transmits high-frequency electromagnetic waves into the ground and receives the backscattered waves reflected from the underground objects [2]. These backscattered waves are then detected by the GPR receiving antenna for post-processing to obtain underground feature maps of subsurface contents. As the GPR equipment scans horizontally above the ground surface, a B-scan image is formed, which shows a two-dimensional cross-sectional view of the underground surface, highlighting the reflectivity of subsurface scatterers. Though effective, these GPR systems are implemented using custom hardware that is costly and often difficult to build due to the requirement of extremely wide bandwidths [3] [2].

To circumvent the GPR cost and size constraints, Software-Defined Radio (SDR) has emerged as a potential wireless research tool that can be rapidly prototyped for various radio applications [4] [5]. Numerous recent studies have tried to exploit the potentials of using SDR in various radar applications including GPR [6] [7]. However, temperature variations and non-ideal behaviour of components, tend to produce IQ-imbalances and phase distortions [8]. IQ-imbalances are the perturbations produced in the amplitude and phase of the received In-phase (I) and Quadrature-phase (Q) signal in direct-conversion receivers [9]. These perturbations distort the received signal and eventually manifest as ghost images in the generated B-scan [9]. Ghost images appear to be as false reflectivity response present at different range bins. This masks the true reflectivity feature maps obtained for an actual buried target, hence increasing the ambiguity in interpreting the corrupted B-scans.

A conventional approach to cater the phase distortions is by calibrating the SDR equipment [8]. The phase errors, however, tend to change with time and temperature, therefore, calibration of SDR has to be carried out periodically [8]. On the other hand, some post-processing techniques also exist to

Second Workshop on Machine Learning and the Physical Sciences (NeurIPS 2019), Vancouver, Canada.

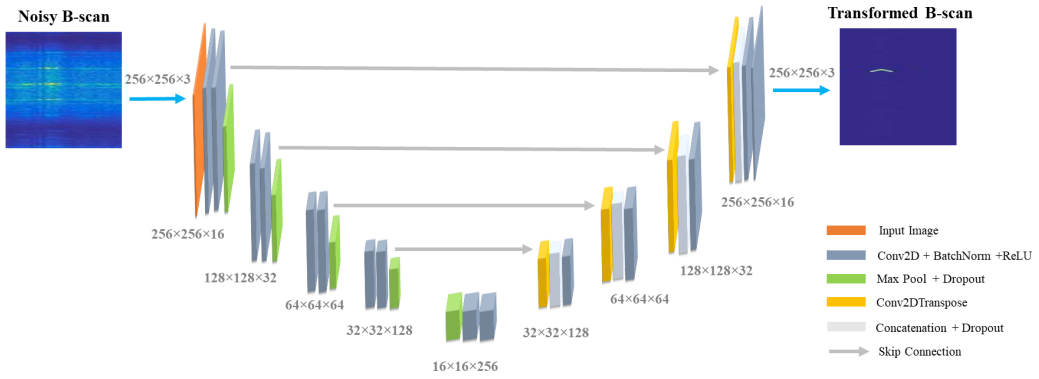

Figure 1: U-Net Network Architecture [13]. U-Net makes use of skip connections from each layer in the encoder and concatenates it with its corresponding layer in the decoder section. This allows the network to retain the localized information content as it gets upsampled in the decoder.

mitigate the effects of IQ-imbalances and phase distortions by applying corrections once the radar image has been formed [9]. However, these techniques could only smear the artifacts and ghost images, without completely removing them from the radar images [9].

Recently, deep learning based approaches have achieved state of the art performance in numerous computer vision and image processing tasks. By leveraging the power of huge training datasets, these techniques have been shown to outperform the conventional signal processing approaches [10] [11].

In this work, we aim to explore a novel post-processing approach, GPRNet, that leverages the potentials of deep learning for transforming the corrupted B-scans generated using SDR based GPR. Through extensive experiments on real B-scans acquired via USRP2943R [12], we demonstrate the effectiveness of deep learning for accurately identifying the presence and depth of a subsurface object from noise corrupted B-scans. To circumvent the issue of data scarcity, we exploit U-Net based architecture that has been shown to produce promising results over the small training dataset [13].

2 Methodology

This section highlights the main steps of training U-Net for transforming the corrupted B-scan images obtained using USRP2943R (SDR from National Instruments [12]). U-Net has been employed due to its ability to give impressive results even for small training datasets [13]. Figure 1 shows the network architecture of U-Net employed for transforming the noisy B-scans.

Let $\boldsymbol{x} \in \mathbb{R}^n$ and $\boldsymbol{x^*} \in \mathbb{R}^n$ represent the corrupted B-scan image and its corresponding ground truth B-scan image, respectively. Our goal is to find a function mapping f_θ that maps a corrupted B-scan $\boldsymbol{x}$ to the estimate $\hat{\boldsymbol{x}}$ of its clean version $\boldsymbol{x^*}$. The function f_θ is modelled by U-Net, where θ represents the weight parameters of the encoder and decoder of the U-Net. During training, the weights of the network are updated by minimizing the Mean Squared Error (MSE) loss between the reconstructed B-scan image $f_\theta(\boldsymbol{x}_\ell)$ and its corresponding ground truth B-scan image $\boldsymbol{x}_\ell^*$. The MSE loss function is mathematically expressed as:

$$\min_{\theta} \quad \sum_{\ell=1}^{L} \frac{1}{L} \|\boldsymbol{x}_\ell^* - f_\theta(\boldsymbol{x}_\ell)\|^2, \tag{1}$$

where, $\ell = 1, 2, ...L$ represent the training data set, and $\|.\|$ denotes the ℓ_2-norm operation.

(a) GPR Scanner (b) Steel Bearing (c) Iron Weight

Figure 2: (a) GPR scanner hardware along with two log periodic antennas [14], each for transmitter and receiver (b) Steel bearing of diameter 7 cm (c) Iron weight object of diameter 10 cm.

3 Experiments

This section describes the experiments conducted for the evaluation of the proposed methodology. To overcome the issue of data scarcity, the dataset have been acquired using the GPR designed on USRP2943R [12]. Multiple B-scans have been generated for different depths and position of subsurface objects shown in Figure 2. Ground truth of noisy B-scans have been generated using MATLAB by simulating the reflectivity response of buried object. A total set of 1700 B-scan images have been generated for the dataset, with train-validate-test ratio of 80-10-10, respectively. U-Net have been trained with a batch size of 4 over 100 epochs, using Adam optimzer..

For comparsion, two different network architectures have also been evaluated in comparison to the presented U-Net on this dataset including a Convolutional Neural Network (CNN) and a Denoising Autoencoder (DAE). CNN model consists of 9 sequential 3×3 convolutional layers whereas DAE consists of 4 sequential 3×3 convolutional layers, each followed by a 2×2 max pooling layer in both the encoder and decoder section of the network. Figure 3 shows the prediction results obtained from each of the three networks. It can be clearly seen that the reconstructed outputs of both the CNN and DAE have no subsurface information content present in them, thus completely failing to serve the purpose. On the other hand, U-Net has shown promising results by accurately predicting the buried object's depth and position in the reconstructed B-scans.

For quantitative analysis of the reconstructed B-scans, we define an evaluation metric, Average Range Error (ARE), that is specifically defined to compute the absolute range or depth error between the predicted range and the actual range from the reconstructed B-scan and its corresponding ground truth, respectively. Range error is computed for each test B-scan and averaged over the entire test dataset. The mathematical expression for computing ARE is expressed below:

$$\text{ARE} = \frac{1}{T} \sum_{t=1}^{T} |R^*[t] - \hat{R}[t]| \tag{2}$$

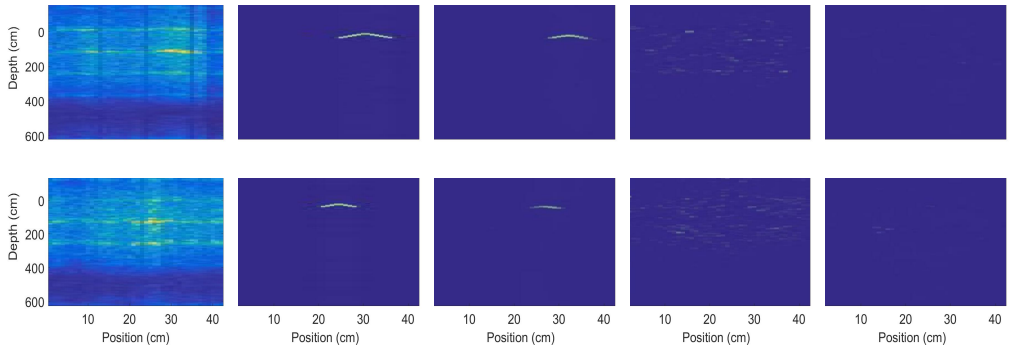

(a) Original (b) Ground Truth (c) UNET (d) CNN (e) DAE

Figure 3: First and second row shows the predicted results of U-Net, CNN and DAE for iron weight and steel bearing, respectively. Both objects were buried 5 cm below the soil surface and 10 cm below the antennas. Note that the reflectivity of a subsurface scatterer typically appears as a hyperbolic curve in B-scans, because its range decreases and increases as the GPR scans towards and away from that scatterer.

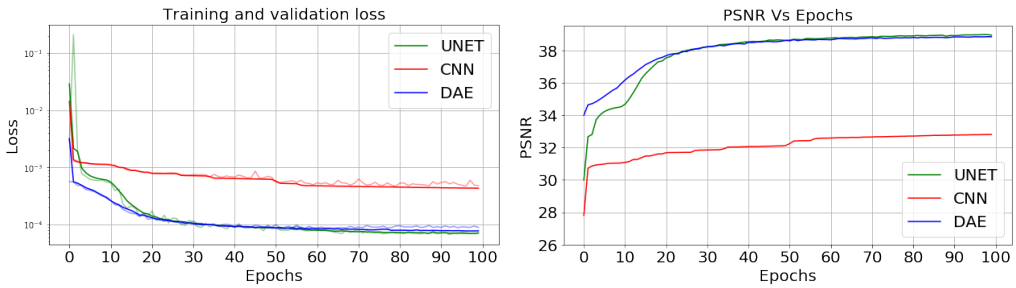

(a) Training Loss (b) PSNR

Figure 4: (a) Training and Validation Loss obtained as a function of training epochs, (b) Plot obtained for average PSNR as a function of training epochs

Where, T is the total number of test B-scan images. $R^*[t]$ and $\hat{R}[t]$ represents the true range and predicted range of scatterer in the t^{th} B-scan image, respectively. Furthermore, the reconstructed B-scans have also been evaluated on the two most commonly used evaluation metrics i.e. Peak Signal to Noise Ratio (PSNR) and Structural Similarity Index (SSIM) [15]. Figure 4 shows the training loss and average PSNR obtained during training for all three networks. Despite, the average PSNR and SSIM for DAE appears to be comparable as that of U-Net, yet U-Net shows better results in its reconstructed B-scans owing to its characteristic architecture that makes use of skip connections from encoder to decoder. This helps to preserve the localized subsurface information in the reconstructed B-scans as it gets upsampled in decoder.

In addition, the U-Net model has been trained using different activation functions including Rectified Linear Unit (ReLU), sigmoid and softmax. Since, ReLU is more sensitive to its inputs [16] [17], it clearly outperforms sigmoid and softmax quantitatively, as shown in Table 1.

Table 1: Table shows the quantitative results including PSNR, SSIM and ARE, evaluated for U-Net, CNN, and DAE. U-Net is further evaluated using different activation functions i.e. ReLU, sigmoid and softmax. Due to unfavourable results, ARE could not be computed for other networks except U-Net.

Network Model	**Activation Function**	**PSNR (dB)**	**SSIM (dB)**	**ARE (cm)**
U-Net	ReLU	37.62	0.99	2.39
	Sigmoid	32.49	0.98	3.35
	Softmax	28.66	0.97	-
CNN	ReLU	36.23	0.96	-
DAE	ReLU	37.33	0.99	-

4 Conclusion and Future Direction

This work has demonstrated the potentials of deep learning as an efficient post-processing technique for mitigating the effects of phase distortions in the B-scans acquired using SDR based GPR. An existing architecture, U-Net, has been shown to provide promising results for transforming the corrupted B-scans that accurately predicts the depth of subsurface object, with an average range error around 2.4 cm only, obtained over a test data of around 150 B-scans. In addition, the proposed U-Net architecture has been shown to outperform CNN and DAE networks by faithfully predicting the subsurface content in transformed B-scans.

While deep learning appears to be a favourable tool for circumventing the effects of phase distortions in B-scans, the scope of this work can be further extended to generalize the model even better by acquiring huge amount of dataset from GPR designed on different SDRs. In addition, incorporating buried objects of different materials in the dataset of B-scans can help to identify multiple buried scatterers and perform classification based on their material. Hence, adding more parameters to the model will allow it to be more useful in extensive applications of subsurface exploration using low cost software-defined radios.

Acknowledgements

The authors would like to acknowledge National Research Program for Universities (NRPU) grant by Higher Education Comission (HEC) Pakistan, for funding this work.

References

[1] Harry M. Jol. *Ground Penetrating Radar Theory and Applications*. Elsevier Science, 2009.

[2] Mark. A. Richards. *Fundamentals of Radar Signal Processing*. McGraw-Hill, 2014.

[3] Andrew Wilkinson, Richard Lord, and Michael Inggs. Stepped-frequency processing by reconstruction of target reflectivity spectrum. pages 101 – 104, 10 1998.

[4] Giuseppe Di Massa1 Antonio Borgia1 Antonio Costanzo1 Gianluca Aloi Pasquale Pace1 Valeria Loscr Sandra Costanzo1, Francesco Spadafora1 and Hugo O. Moreno. Potentialities of usrp-based software defined radar systems. *Progress In Electromagnetics Research B*, 2013.

[5] K Gallagher A Martone K Sherbondy R Narayanan B Kirk, J Owen. Development of a software-defined radar. 2017.

[6] S. C. Carey and W. R. Scott. Software defined radio for stepped-frequency, ground-penetrating radar. In *2017 IEEE International Geoscience and Remote Sensing Symposium (IGARSS)*, pages 4825–4828, July 2017.

[7] Peng Liu, Jesus Mendoza, Hanxiong Hu, Peter Burkett, Julio Urbina, Sridhar Anandakrishnan, and Sven Bilén. Software-defined radar systems for polar ice-sheet research. *IEEE Journal of Selected Topics in Applied Earth Observations and Remote Sensing*, 12:803–820, 03 2019.

[8] Ettus Knowledge Base. Synchronization and mimo capability with usrp devices — ettus knowledge base. `https://kb.ettus.com/index.php?title=Synchronization_and_MIMO_Capability_with_USRP_Devices&oldid=3524`, 2017.

[9] A. W. Doerry. Balancing i/q data in radar range-doppler images. `https://doi.org/10.1117/12.2075745`, 2015.

[10] Huiming Li. Deep learning for image denoising. 2014.

[11] Guo B Qin Q Chen R. Wang R, Xiao X. An effective image denoising method for uav images via improved generative adversarial networks. *A Sensors (Basel)*, (2018;18(7):1985), 06 2018.

[12] National Instruments Knowledge Base. Usrp-2943 specifications - national instruments. `http://www.ni.com/pdf/manuals/374193d.pdf`, 2017.

[13] Olaf Ronneberger, Philipp Fischer, and Thomas Brox. U-net: Convolutional networks for biomedical image segmentation. *CoRR*, abs/1505.04597, 2015.

[14] Ettus Research contributors. Lp0965 log periodic antenna. `https://www.ettus.com/all-products/lp0965/`.

[15] Zhou Wang, Alan Bovik, Hamid Sheikh, and Eero Simoncelli. Image quality assessment: From error visibility to structural similarity. *Image Processing, IEEE Transactions on*, 13:600 – 612, 05 2004.

[16] Vinod Nair and Geoffrey E. Hinton. Rectified linear units improve restricted boltzmann machines. In *Proceedings of the 27th International Conference on International Conference on Machine Learning*, ICML'10, pages 807–814, USA, 2010. Omnipress.

[17] Chigozie Nwankpa, Winifred Ijomah, Anthony Gachagan, and Stephen Marshall. Activation functions: Comparison of trends in practice and research for deep learning. *CoRR*, abs/1811.03378, 2018.